CrossMark

RESEARCH PAPER

# Mesoporous silicas with covalently immobilized β-cyclodextrin moieties: synthesis, structure, and sorption properties

**Nadiia V. Roik** (ID) · **Lyudmila A. Belyakova** ·
**Iryna M. Trofymchuk** · **Marina O. Dziazko** ·
**Olena I. Oranska**

**Abstract** Mesoporous silicas with chemically attached macrocyclic moieties were successfully prepared by sol-gel condensation of tetraethyl orthosilicate and β-cyclodextrin-silane in the presence of a structure-directing agent. Introduction of β-cyclodextrin groups into the silica framework was confirmed by the results of IR spectral, thermogravimetric, and quantitative chemical analysis of surface compounds. The porous structure of the obtained materials was characterized by nitrogen adsorption-desorption measurements, powder X-ray diffraction, transmission electron microscopy, and dynamic light scattering. It was found that the composition of the reaction mixture used in β-cyclodextrin-silane synthesis significantly affects the structural parameters of the resulting silicas. The increase in (3-aminopropyl)triethoxysilane as well as the coupling agent content in relation to β-cyclodextrin leads ultimately to the lowering or complete loss of hexagonal arrangement of pore channels in the synthesized materials. Formation of hexagonally ordered mesoporous structure was observed at molar composition of the mixture 0.049 TEOS:0.001 β-CD-silane:0.007 CTMAB:0.27 $NH_4OH$:7.2 $H_2O$ and equimolar ratio of components in β-CD-silane synthesis. The sorption of alizarin yellow on starting silica and synthesized materials with chemically attached β-cyclodextrin moieties was studied in phosphate buffer solutions with pH 7.0.

Experimental results of the dye equilibrium sorption were analyzed using Langmuir, Freundlich, and Redlich-Peterson isotherm models. It was proved that the Redlich-Peterson isotherm model is the most appropriate for fitting the equilibrium sorption of alizarin yellow on parent silica with hexagonally arranged mesoporous structure as well as on modified one with chemically immobilized β-cyclodextrin groups.

## Introduction

Among such "host" molecules as crown ethers, functionalized cyclophanes, cryptands, cyclodextrins (CDs) have unique potential due to their ability to form inclusion complexes with a wide variety of organic and inorganic substances (Hegeson et al. 1973; Lehn 1978, 1995; Pedersen 1967; Steed and Atwood 2009; Szejtli 1998). Encapsulation of "guest" molecules leads to the enhancement of their solubility; prolongs half-life by stabilization against the degradative effects of oxidation, visible or UV light, and heat treatment; and provides control of volatility and sublimation (Dodziuk 2006). Stability of inclusion complexes can differ substantially in dependence of chemical and geometrical compatibility between "host" and "guest" molecules. Therefore, CDs have promising potential in drug delivery processes (Agrawal and Gupta 2012), molecular recognition

N. V. Roik (✉) · L. A. Belyakova · I. M. Trofymchuk · M. O. Dziazko · O. I. Oranska
Chuiko Institute of Surface Chemistry of NAS of Ukraine, 17 General Naumov Str, Kyiv 03164, Ukraine
e-mail: roik_nadya@ukr.net

(Liu et al. 2004a, b), and separation techniques (Shpigun et al. 2003; Schneiderman and Stalcup 2000). Although separation of CD inclusion complexes is complicated by their high solubility in water, this difficulty may be potentially overcome by transformation of CD moieties into insoluble form. Different techniques are used for this purpose including cross-linking of CD molecules, immobilization on the surface of organic and inorganic polymers as well as metal nanoparticles (Concheiro and Alvarez-Lorenzo 2013; Gidwani and Vyas 2015; Lala et al. 2011; Li et al. 2010, 2013; Liu et al. 2000; Patel and Deshpande 2014; Tiwari et al. 2010). From the variety of potential β-CD carriers, MCM-41 silica could be considered as an ideal one because it has high chemical, thermal, and hydrolytic stability; good biocompatibility; pore diameter ranging from 2 to 10 nm; large pore volume; and surface area up to 1200 $m^2 g^{-1}$. Moreover, surface functional coverage can be easily modified to attain desired chemical properties due to the presence of highly reactive silanol groups. Therefore, the successful attempts to immobilize β-CD moieties on MCM-41 surface by sol-gel synthesis (Bibby and Mercier 2003; Hug and Marcier 2001; Liu et al. 2004a, b) or grafting technique (Bai et al. 2004; Chen et al. 2002; Fujimura et al. 1983; Feng et al. 2000; Gong and Lee 2003; Kawaguchi et al. 1983; Lai and Ng 2003; Liu et al. 2005a, b; Phan et al. 1999; Palaniappan et al. 2006; Phan et al. 2000; Roik and Belyakova 2011; Shvets and Belyakova 2015; Xu et al. 2011; Zhang et al. 1999) were undertaken with the aim to form effective and highly selective centers for sorption of organic compounds. Chemical immobilization of cyclic oligosaccharide by sol-gel polycondensation approach has some advantages in comparison with postsynthetic modification of

MCM-41 surface. The most essential of them is uniform distribution of β-CD-containing functional groups in silica matrix. Preferential localization of oligosaccharide functionalities on the outer surface of silica particles and at the entrances to the pores which takes place at postsynthetic treatment of mesoporous materials with pore diameter smaller than 5 nm (Hug and Marcier 2001; Phan et al. 2000) is undesired because it can cause blocking and poor accessibility of pore channels for large sorbed molecules (Salis et al. 2010).

In this paper, a simple strategy for the synthesis of β-CD-functionalized silica materials with hexagonally ordered mesoporous structure was proposed. First, β-CD-silane was prepared via coupling of cyclic oligosaccharide to (3-aminopropyl)triethoxysilane (APTES) with 1,1′-carbonyldiimidazole (CDI) participation (Scheme 1). Then, base-catalyzed condensation of synthesized silane with tetraethyl orthosilicate (TEOS) was realized in the presence of cetyltrimethylammonium bromide (CTMAB) as a structure-directing agent (Scheme 2). To elucidate contribution of β-CD macrocycles in the removing of dye from neutral aqueous solutions, sorption studies of alizarin yellow (AY) were carried out on parent and modified silicas with chemically attached oligosaccharide moieties.
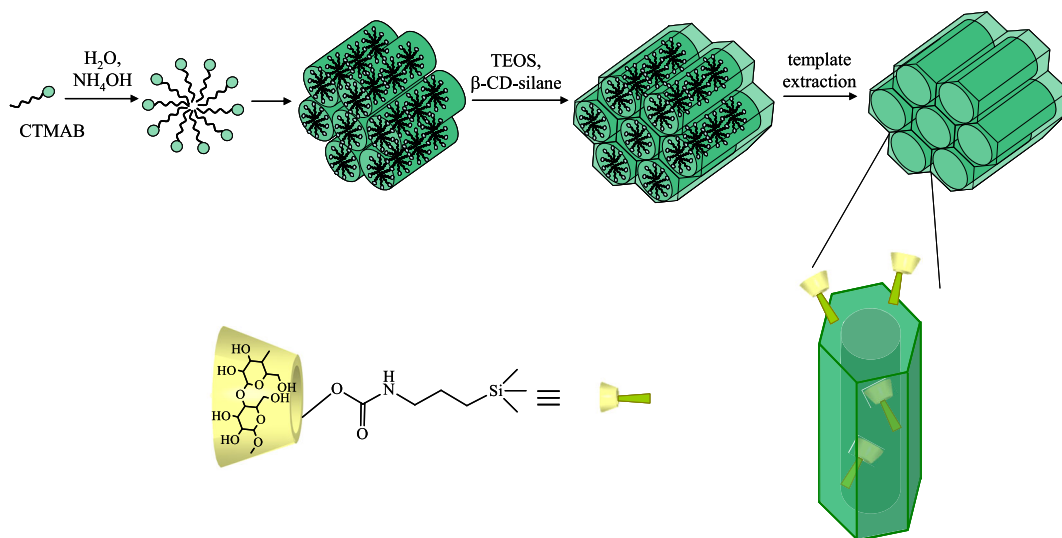
## Materials and methods

### Materials

Tetraethyl orthosilicate from "Merck" (≥ 99%), (3-aminopropyl)triethoxysilane from "Merck" (≥ 99%),
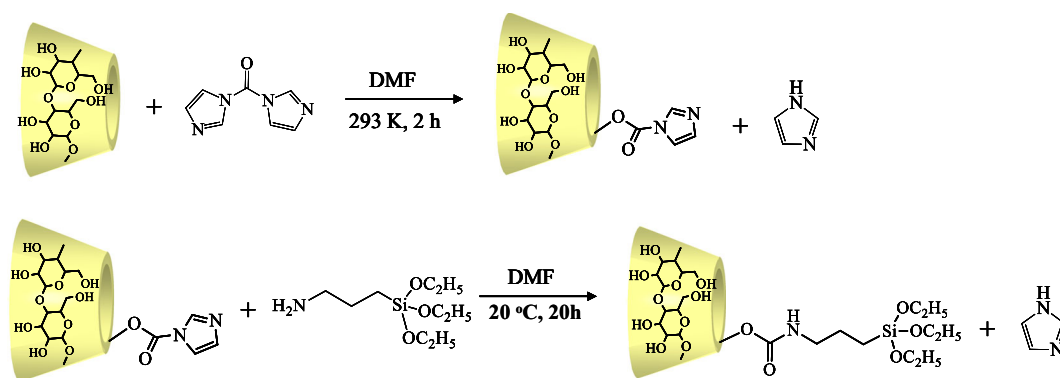


**Scheme 1** Synthesis of β-cyclodextrin-containing silane

**Scheme 2** Sol-gel synthesis of β-cyclodextrin-containing silica

β-cyclodextrin from "Fluka" (≥99%), 1,1′-carbonyldiimidazole from "Merck" (≥98%), and cetyltrimethylammonium bromide from "Merck" (≥97%) were used as received. $N,N'$-dimethylformamide (DMF) from "Reakhim" (pure analytical) was dried for 72 h by using 4-Å molecular sieves. Alizarin yellow sodium salt, disubstituted sodium phosphate, and monosubstituted potassium phosphate were obtained from "Reakhim" (pure analytical) and used without additional purification as well as hydrochloric acid 37% and ethanol 96% from "Reakhim" (chemical grade).

Synthesis of β-CD-silanes

Covalent attachment of highly reactive triethoxysilyl groups to β-CD molecule was realized by standard coupling procedure (Staab 1962) proceeding through carbamate linkage formation between cyclic oligosaccharide and APTES with CDI participation. For β-CD-silane synthesis, the batch of β-CD (0.001 mol) was placed into the flask with 15 ml of DMF, dissolved, and treated with solution of CDI (0.00105, 0.00315, or 0.00525 mol) in DMF. Activation of oligosaccharide hydroxyl groups was achieved by stirring the reaction mixture at 293 K for 2 h. Then, APTES (0.001, 0.003, or 0.005 mol) was added into the flask to link with activated β-CD. The solution was stirred at 20 °C for 20 h and used in sol-gel synthesis of corresponding β-CD-containing silica materials.

Templated sol-gel synthesis of MCM-41 silica material and β-CD-functionalized silicas

MCM-41 silica material was synthesized by base-catalyzed sol-gel condensation of TEOS in the presence of quaternary ammonium salt as structure-directing agent (Roik and Belyakova 2013). The precipitated white product was kept in the reaction mixture with stirring for 2 h, then transferred to a polypropylene bottle for hydrothermal treatment at 100 °C for 24 h. After that, the synthesized silica was filtered, washed with 100 ml of deionized water, and dried in air at 100 °C for 3 h.

The sol-gel procedure previously developed by Grun et al. (1997) was modified to prepare β-CD-functionalized mesoporous silicas of MCM-41-type. Briefly, weighted amount of the surfactant structure-directing agent CTMAB (0.007 mol) was dissolved under vigorous stirring in distilled water (7.2 mol). After the addition of 25% aqueous ammonium (0.27 mol), TEOS (0.049 mol) and a mixture obtained in β-CD-silane synthesis were poured into the flask under continuous stirring at 20 °C. The reaction slurry was then agitated at 20 °C for 2 h, transferred into the polypropylene bottle, and heated at 100 °C for 24 h. The precipitated product was filtered, rinsed with deionized water, and dried in air at 100 °C for 2 h. For clarity, synthesized β-CD-functionalized silica materials were denoted as CD-SiO$_2$/CD-SiO$_2$-1, CD-SiO$_2$-2, and CD-SiO$_2$-3, respectively.

The surfactant (CTMAB) was extracted from pore channels of mesoporous organosilicas by stirring the

batch of the as-synthesized material (1 g) with a solution of hydrochloric acid (8 ml) and ethanol (92 ml) at 25 °C for 24 h. After separation of silica particles from the solution by filtration, the extraction procedure was repeated two more times. The resulting mesoporous silica was filtered, washed with deionized water until the absence of halogen ions in the filtrate (negative probe with silver nitrate), and dried in the air at 100 °C for 5 h.

## Characterization of silica materials

The IR spectra of synthesized silica materials were recorded at room temperature using a Thermo Nicolet NEXUS FT-IR spectrophotometer in frequency range from 4000 to 1200 cm$^{-1}$ with a resolution of 2 cm$^{-1}$ and 32 scans for each run (Stuart 2004; Larkin 2011; Alahmadi et al. 2014).

Thermogravimetric analysis was carried out on a Perkin Elmer 7 series thermal analyzer. Weighed powdered silica samples were used in each test. Temperature varied from 25 to 900 °C, and heating rate was 10 °C min$^{-1}$ (Gabbott 2008; Chong and Zhao 2003; Shvets and Belyakova 2015).

The content of β-CD moieties introduced into the silicas in the process of sol-gel synthesis was estimated also by acid hydrolysis of surface β-CD-containing groups to glucose and their subsequent determination by color reaction with potassium ferricyanide (Korenman 1970; Roik and Belyakova 2011).

The amount of 3-aminopropyl groups on the surface of β-CD-functionalized silicas was determined by the multibatch potentiometric titration (Helfferich 1995; Belyakova et al. 2006). For this, the batches of silica materials (0.5 g) were placed in 50-ml round-bottom glass flasks and 0−25 ml of aqueous solutions of 0.01 M HCl were added. In all experiments, the volume of the aqueous solutions was 25 ml. The prepared suspensions were stirred by a magnetic stirrer at 20 °C for 24 h to attain equilibrium. pH values of the starting and equilibrium solutions were measured by an Ionometer I-120.1 that was calibrated for optimal precision using standard buffer solution of pH 1.68 and pH = 6.86. The content of protonated 3-aminopropyl groups on the surface of mesoporous silicas at various pH solutions was calculated by the formula:

$$[NH_2] = \frac{\left(10^{-pH_1} - 10^{-pH_2}\right) \cdot V}{m},$$ (1)

where [$NH_2$]—content of protonated 3-aminopropyl groups of mesoporous silica, moles per·gram; pH$_1$ and pH$_2$—pH of the starting and equilibrium solutions, respectively; V—volume of the solution, liter; and m—batch of mesoporous silica, grams.

The total static capacity of β-CD-functionalized silicas corresponds to the content of grafted 3-aminopropyl groups.

The porous structure of silica materials was characterized by low-temperature adsorption-desorption of nitrogen at $T = -196$ °C using Kelvin-1042 Sorptometer. The silicas were first outgassed under vacuum at 140 °C for 20 h and then analyzed in the region of relative pressures from 0.06 to 0.99 in increment of 0.015. Specific surface area ($S_{BET}$) was evaluated by the Brunauer-Emmet-Teller (BET) method, pore diameter (D) was calculated by the nonlocal density functional theory (NLDFT), and pore volume ($V_p$) was determined at $p/p_o = 0.95$ (Kruk and Jaroniec 1999; Kim et al. 2010).

X-ray diffraction spectra were registered by using the diffractometer DRON-4-02 with monochromatic CuK$_\alpha$ emission ($\lambda = 0.15418$ nm) and nickel filter (Kruk and Jaroniec 1999; Kim et al. 2010).

Hydrodynamic size of silica particles was evaluated by dynamic light scattering (DLS) using Malvern Zetasizer (Version 7.11). All measurements were performed for diluted aqueous suspensions of synthesized silica materials (0.1 mg ml$^{-1}$) and repeated eight times at 25 °C (Kaasalainen et al. 2017; Patil et al. 2011).

The transmission electron microscopy (TEM) images of mesoporous silicas were registered on a JEM-100CXII electron microscope at 200 kV. Carbon-coated copper grids were used as the silica holders (Kruk et al. 2000).

## Adsorption studies

To perform adsorption kinetic experiment, weighted amounts of MCM-41 or β-CD-containing silica (0.01 g) were placed in 50-ml round-bottom glass flasks, and 10 ml of 0.323 mM alizarin yellow phosphate buffer solution with pH 7.0 was added to each of them. The flasks were capped and placed on a mechanical shaker at 20 °C. After the suspensions were shaken for predetermined contact time, the aliquots of the supernatant solutions were taken for further UV-vis spectrophotometric analysis with a Specord M-40. The concentration of the dye was evaluated from optical density of

absorption band at 374 nm using the calibration curve plotted in the concentration range of AY from 0.032 to 0.323 mM. The amount of AY sorbed on silica at time $t$ was calculated by the formula:

$$A_t = \frac{(C_o - C_t) \cdot V}{m}, \qquad (2)$$

where $A_t$—sorbed dye content at time $t$, millimoles per·gram; $C_o$ and $C_t$—concentrations of the dye in a solution at initial moment and at time $t$, correspondingly, millimoles per·liter; $V$—volume of the solution, liter; and $m$—weight of silica used, grams.

Equilibrium sorption studies were performed by the multibatch method. For this, a set of phosphate buffer solutions with various concentrations of AY (0.129−0.323 mM) and pH 7.0 was prepared. The batches of silica materials (0.01 g) were placed in 50-ml round-bottom glass flasks, poured with prepared AY solutions (10 ml), and shaken at 20 °C for equilibrium attainment. Thereafter, the supernatant solutions were separated by filtering through a 0.22-μm PVDF syringe filter and analyzed using UV-vis spectrophotometer at wavelength 374 nm. The amount of AY sorbed on silica at equilibrium was calculated as described above.

## Results and discussion

### Synthesis of β-CD-functionalized silicas

To provide homogeneous allocation of β-cyclodextrin groups on the surface of mesoporous silica, template-assisted sol-gel condensation of β-CD-silane and TEOS in water-ammonium medium was realized. In this work, APTES was employed to introduce highly reactive alk-oxy groups in β-CD structure via coupling reaction with CDI participation (Scheme 1). Usually, during synthesis of cyclic oligosaccharide derivatives, isolation of the resulting product is achieved by its precipitation in excess of acetone (Eguchi et al. 2005) or ether (Mondjinou et al. 2013; Cai et al. 2011), evaporation of reaction mixture (Liu et al. 2004a, b) as well as purification by column chromatography (Yano et al. 2001). All these procedures are time and effort consuming as they require the use of additional reagents and equipment. Therefore, two approaches of organosilica matrix preparation were proposed in the present work,

and the structural parameters of the obtained materials were compared to find the most suitable method of synthesis. In accordance with the first of them, β-CD-silane precipitated in acetone with subsequent solvent removing under reduced pressure was introduced in sol-gel synthesis. The second approach involves the use of β-CD-silane solution without preliminary isolation of the resulting product from the reaction mixture. Since amide bonds which retain β-cyclodextrin moieties on silica surface are sensitive to the pH of the reaction slurry, it can be expected that their partial hydrolysis at hydrothermal treatment of silica materials in water-ammonium medium in the process of synthesis may occur (Dittert and Higuchi 1963). To achieve a stronger retention of cyclic oligosaccharide in the silica surface, the additional quantity of anchoring groups was introduced into the β-CD-silane by the change in β-CD:APTES molar ratio.

### Structure of β-CD-functionalized silicas

Immobilization of β-CD-containing groups in silica materials was evidenced by IR spectral and chemical analysis of functionalized silicas. Figure 1 represents the IR spectra of silicas prepared by sol-gel condensation of TEOS and β-CD-silanes with various contents of anchoring groups. The IR spectrum of CD-SiO$_2$ was compared to CD-SiO$_2$-1 in order to emphasize the fact that using the reaction mixture obtained from silane synthesis without preliminary isolation of the resulting product does not influence the IR spectral characteristics and hence the chemical composition of the final silica material surface. Indeed, in the IR spectra of both silicas (Fig. 1, curves 1 and 2), the absorption bands at 3000−2500 cm$^{-1}$ corresponding to the valence vibrations of the C–H bond in the alkyl and glycosyl groups of grafted compounds are registered. The band with a maximum at 1450 cm$^{-1}$ is assigned to the bending vibrations of the C−H, H−C−H, and C−O−H bonds; the bands at 1413 and 1391 cm$^{-1}$ belong to the bending vibrations of the C−C–H and C−O−H bonds in the chemically immobilized groups, correspondingly. Moreover, the characteristic absorption band at 1540 cm$^{-1}$ belonging to the deformation vibrations of the N–H bond in the secondary amino groups of β-CD-functionalized silica materials is clearly shown. As can be seen from the IR spectra of CD-SiO$_2$ and CD-SiO$_2$-1, absorption bands attributed to the deformation vibrations of the N–H bond in the residual primary amino
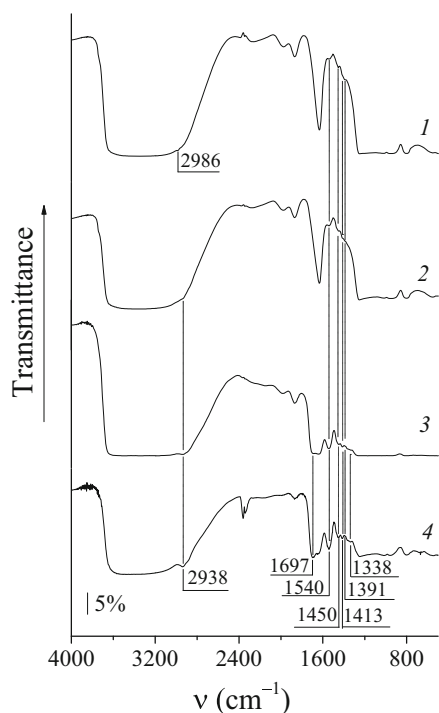
**Fig. 1** IR spectra of β-cyclodextrin-containing silicas: CD-SiO$_2$ (*1*), CD-SiO$_2$-1 (*2*), CD-SiO$_2$-2 (*3*), and CD-SiO$_2$-3 (*4*)

groups as well as valence vibrations of the C=O bond in the carbamate linkage of synthesized silicas expected close to 1560−1640 and 1700 cm$^{-1}$ (Nakanishi 1962), respectively, are not registered because of their overlapping with the strong signal attributed to the deformation vibrations of the O–H bond in adsorbed water. Introduction of oligosaccharide moieties into the silica framework was confirmed by the results of quantitative chemical analysis of β-CD-functionalized silicas (Table 1). The increase of β-CD:APTES molar ratio up to 1:3 and 1:5 in β-CD-silane synthesis leads to the substantial enhancement of the content of surface amino and β-

cyclodextrin groups in the obtained CD-SiO$_2$-2 and CD-SiO$_2$-3 silicas (Table 1). The position of characteristic absorption bands in the IR spectra of β-CD-containing silica materials with higher content of functional groups remains the same. However, their intensities are increased noticeably confirming the successful anchoring of the greater amounts of amino- and β-CD-containing groups in the surface layer of synthesized materials. Furthermore, clearly defined absorption bands at 1697 and 1338 cm$^{-1}$ belonging to the valence vibrations of the C=O bond in the carbamate linkage and stretching vibrations of the C−O as well as bending vibrations of the C−O−H bonds in β-CD-functionalized silica materials are shown (Fig. 1, curves *3* and *4*). In other words, IR spectroscopy data can serve as evidence of the chemical immobilization of β-cyclodextrin groups on the silica surface.

Table 1 shows the results of quantitative chemical analysis of silicas modified with β-cyclodextrin. The immobilized β-cyclodextrin is removed from the surface of synthesized β-cyclodextrin-containing silicas only by acid hydrolysis. This is additional proof of its chemical immobilization in silica matrices. Synthesized β-CD-silicas contain in their structures also 3-aminopropyl radicals. Hence, the obtained results indicate the successful chemical immobilization of β-CD-containing moieties along with 3- aminopropyl ones on the silica surface.

Figure 2 shows the results of thermal analysis of β-cyclodextrin-containing silicas. For comparison, in Fig. 3, the results of thermal analysis of individual β-cyclodextrin and aminopropylsilica material with [−(CH$_2$)$_3$NH$_2$] = 0.51 mmol g$^{-1}$ and $S_{BET}$ = 523 m$^2$ g$^{-1}$ are presented. On the curves of differential thermal analysis (DTA) for β-cyclodextrin-containing silicas, there are one endo- and two exothermic effects

**Table 1** Chemical composition of β-cyclodextrin-containing silica surface

| Silica material | Content of surface groups | | | | | |
|---|---|---|---|---|---|---|
| | Chemical analysis | | | | Thermogravimetric analysis | |
| | [β-CD], mmol·g$^{-1}$ | [β-CD], μmol·m$^{-2}$ | [NH$_2$], mmol·g$^{-1}$ | [NH$_2$], μmol·m$^{-2}$ | [β-CD], mmol·g$^{-1}$ | [β-CD], μmol·m$^{-2}$ |
| CD-SiO$_2$ | 0.01 | 0.01 | 0.04 | 0.05 | 0.01 | 0.01 |
| CD-SiO$_2$-1 | 0.02 | 0.02 | 0.05 | 0.06 | 0.03 | 0.04 |
| CD-SiO$_2$-2 | 0.07 | 0.14 | 0.11 | 0.21 | 0.09 | 0.18 |
| CD-SiO$_2$-3 | 0.10 | 0.21 | 0.12 | 0.26 | 0.13 | 0.28 |
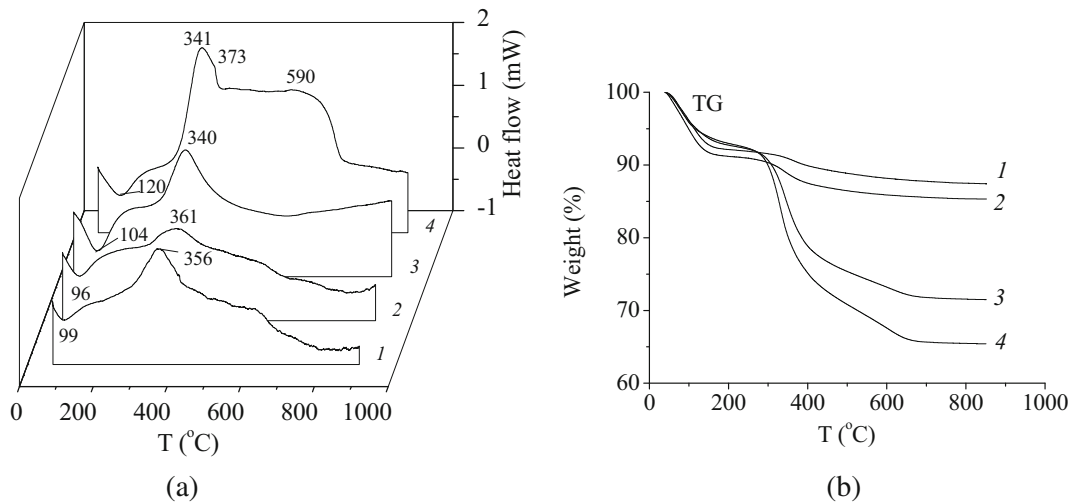
Fig. 2 The curves of differential thermal analysis DTA (**a**) and thermogravimetric analysis TG (**b**) for CD-SiO$_2$ (*1*), CD-SiO$_2$-1 (*2*), CD-SiO$_2$-2 (*3*), and CD-SiO$_2$-3 (*4*)

accompanied by mass loss on the curves of thermogravimetric analysis (TG). At the temperature of 96−120 °C, adsorbed water (Tmax = 101 °C for aminopropylsilica) and water in the β-cyclodextrin cavity (Tmax = 125 °C for the individual β-cyclodextrin) are removed from the surface of β-cyclodextrin-containing silicas. The increase in the content of β-cyclodextrin in the silica materials (Table 1) results in a shift of the endothermic effect to higher temperatures (Fig. 2a). Two exoeffects on the DTA curves for β-cyclodextrin-containing silicas (Fig. 2a) are accompanied by mass loss on the TG curves (Fig. 2b) in temperature intervals 300−400 and 450−700 °C. It is clearly seen that an increase in the content of β-cyclodextrin and 3-aminopropyl functional groups leads

to an increase in mass loss of β-cyclodextrin-containing silicas in these temperature regions. Comparison of thermograms of individual β-cyclodextrin, β-cyclodextrin-containing silicas, and aminopropylsilica gives rise to a conclusion that the destruction of immobilized β-cyclodextrin groups (destruction of alcohol groups and glucopyranose cycles) occurs at about 300 °C. After that, the thermal destruction of imino- and aminopropyl groups (350 °C) begins (Belyakov et al. 2005; Belyakova et al. 2005). Above 400 °C, the oxidative destruction of the carbohydrate residues of the β-cyclodextrin ends, and about 600 °C, the methylene chains of amino- and iminopropyl groups of the bifunctional β-cyclodextrin-containing silicas are destroyed. The content of chemically immobilized β-cyclodextrin
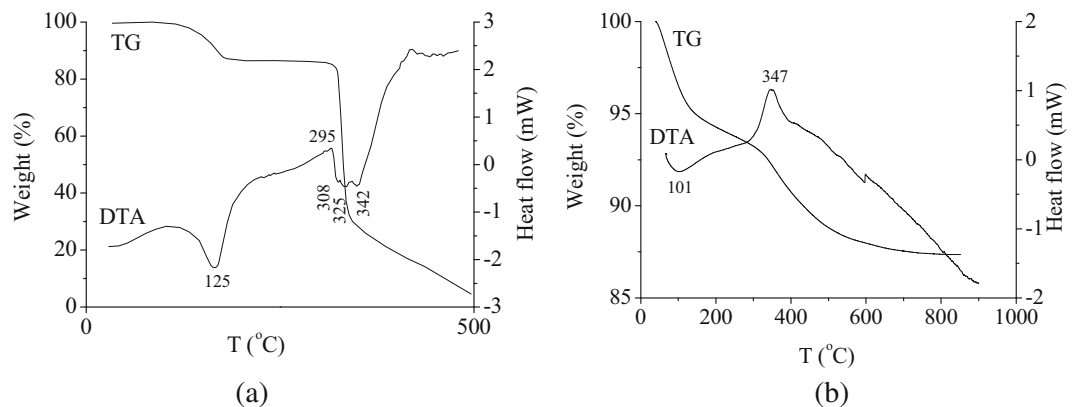


Fig. 3 Thermal analysis of β-cyclodextrin (**a**) and aminopropylsilica (**b**)

determined from the results of thermogravimetric analysis is consistent with the data of quantitative chemical analysis of the synthesized silicas (Table 1).

In the present paper, several techniques like X-ray diffraction, low-temperature adsorption-desorption of nitrogen, and TEM analysis were applied to elucidate the influence of β-CD:APTES molar ratio in β-CD-silane synthesis on the porous structure of corresponding β-CD-functionalized organosilicas. As can be seen from Fig. 4, intensive low-angle reflex at 2.15 $2\theta$ assigned to the (100) plane is registered in the diffractograms of CD-SiO$_2$ and CD-SiO$_2$-1. Moreover, high-angle reflexes at 3.70, 4.30 and 3.75, 4.25 $2\theta$ attributed to the (110) and (200) planes in CD-SiO$_2$ and CD-SiO$_2$-1 silicas, correspondingly, are clearly shown (Fig. 4, curves 1 and 2). Their presence in the diffractograms of silica materials evidences the formation of two-dimensional periodic hexagonal lattice typical for MCM-41. Coincidence of diffraction peaks corresponding to the (100) plane of silicas prepared by the use of purified and as-synthesized β-CD-silanes confirms the equal interplanar distances $d$ in these materials. Obviously, the presence of imidazole which is a by-product of the coupling reaction between β-CD and APTES (Scheme 1) in the sol-gel synthesis does not have noticeable effect on the structure of the resulting silica material.

Comparison of the X-ray diffraction patterns of CD-SiO$_2$-1, CD-SiO$_2$-2, and CD-SiO$_2$-3 silicas indicates that the intensity of (100) reflection decreases several times as the content of anchoring groups in β-CD-silane

becomes higher (Fig. 4, curves 2−4). At the same time, the higher order reflections (110) and (200) do not appear in the diffractograms of CD-SiO$_2$-2 and CD-SiO$_2$-3. Obviously, co-condensation of TEOS with β-CD-silanes obtained at high molar ratio between β-CD and APTES leads to the formation of organosilicas with less ordered mesoporous structure than in the case of CD-SiO$_2$-1. The structural parameters of synthesized materials calculated from the X-ray diffraction data are summarized in Table 2.

The low-temperature nitrogen adsorption-desorption isotherms as well as the pore size distributions of β-CD-functionalized silica materials is shown in Fig. 5a, b. It can be seen that the isotherm curves of CD-SiO$_2$ and CD-SiO$_2$-1 materials are very similar (Fig. 5a, curves 1 and 2). A linear increase in nitrogen adsorption which is observed at low relative pressures ($p/p_o < 0.3$) can be attributed to the monolayer formation on mesoporous walls. It is followed by the sharp enhancement in the quantity of adsorbed nitrogen at relative pressures above 0.3 (Fig. 5a, curves 1 and 2) due to the capillary condensation of adsorbate in mesopores with narrow size distribution (Fig. 5b, curves 1 and 2).

The involvement of β-CD-silanes obtained at high β-CD:APTES molar ratio into the sol-gel co-condensation process results in organosilica materials with less uniform pore structure. As shown in Fig. 5a, the capillary condensation of nitrogen in mesopores of CD-SiO$_2$-2 and CD-SiO$_2$-3 takes place in a broad range of relative pressures evidencing the formation of a complex and multimodal pore system. Indeed, the pore size distributions determined using the NLDFT theory clearly demonstrate that mesopores of several diameters are prevailing in the synthesized materials (Fig. 5b, curves 3 and 4). It can be suggested that the appearance of pores with diameter higher than 3.9 nm (Table 2) can be caused by partial degradation of the walls between individual channels of
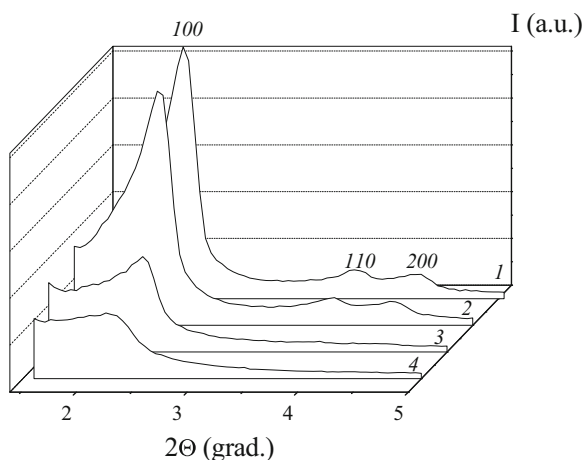


**Fig. 4** X-ray diffraction patterns of CD-SiO$_2$ (*1*), CD-SiO$_2$-1 (*2*), CD-SiO$_2$-2 (*3*), and CD-SiO$_2$-3 (*4*)

**Table 2** Structural parameters of β-cyclodextrin-containing silica materials

| Silica | $d_{100}$, nm | $a$, nm | $S_{BET}$, m$^2$·g$^{-1}$ | $D$, nm | $V$, cm$^3$·g$^{-1}$ |
|---|---|---|---|---|---|
| CD-SiO$_2$ | 4.11 | 4.75 | 802 | 3.9; 5.1 | 1.38 |
| CD-SiO$_2$-1 | 4.11 | 4.75 | 812 | 3.9; 5.1 | 1.06 |
| CD-SiO$_2$-2 | 3.93 | 4.54 | 512 | 2.5; 3.3; 5.1 | 0.60 |
| CD-SiO$_2$-3 | 4.11 | 4.74 | 457 | 2.4; 3.1; 4.7 | 0.69 |

**Fig. 5** Nitrogen adsorption-desorption isotherms (**a**) and pore size distributions (**b**) for CD-SiO$_2$ (*1*), CD-SiO$_2$-1 (*2*), CD-SiO$_2$-2 (*3*), and CD-SiO$_2$-3 (*4*)
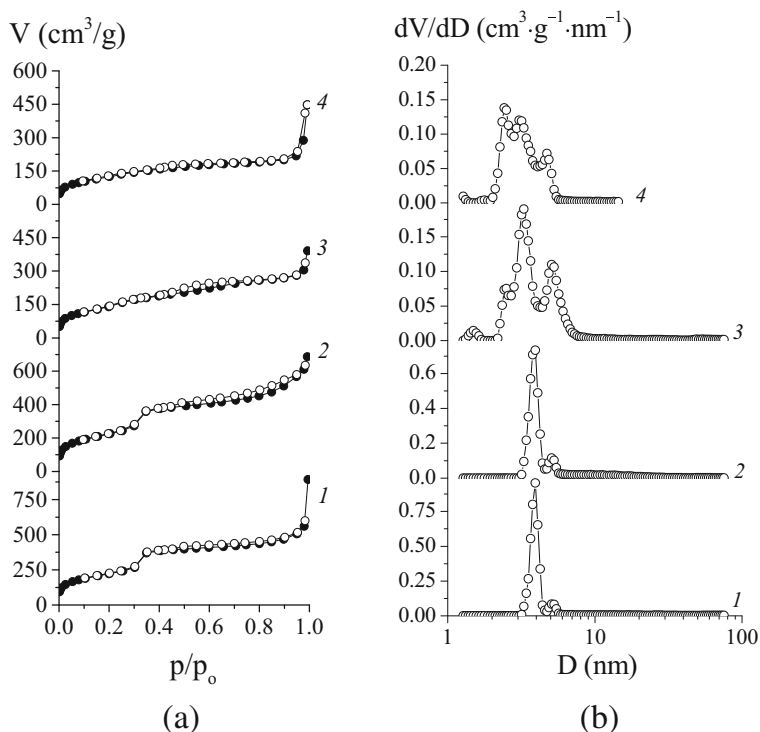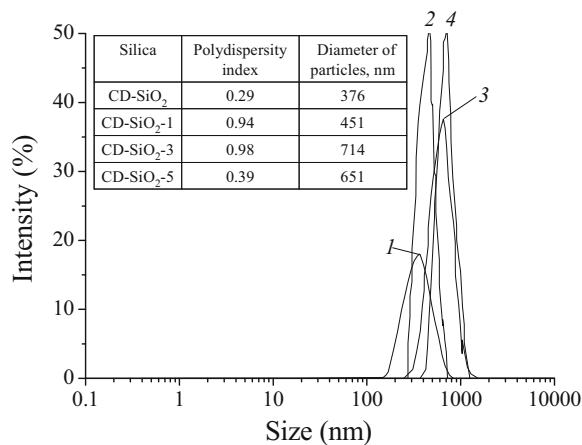


pores in the process of postsynthetic treatment carried out at 100 °C in the medium of ammonia.

The structural parameters of synthesized mesoporous organosilica materials such as specific surface area calculated from the linear region of nitrogen monolayer adsorption using multipoint BET method, average pore diameter evaluated by applying the NLDFT theory (equilibrium model), and total pore volume calculated from the amount of adsorbed nitrogen at a relative pressure equal to 0.99 are summarized in Table 2.

The comparison of results obtained by low-temperature nitrogen adsorption-desorption and X-ray diffraction analyses indicates that β-CD-containing silica materials with hexagonally arranged mesoporous structure and commensurable structural parameters can be prepared by the use of purified β-CD-silane as well as β-CD-silane solution containing the by-product imidazole. However, the increase of anchoring group content in β-CD-silane used in sol-gel synthesis leads to the formation of organosilica framework with less arranged multimodal pore system. Moreover, the values of specific surface area and total pore volume for CD-SiO$_2$, CD-SiO$_2$-1, CD-SiO$_2$-2, and CD-SiO$_2$-3 silicas decrease from 1.38 to 0.69 cm$^3$ g$^{-1}$ and from 802 to 457 m$^2$ g$^{-1}$, correspondingly (Table 2).

Particle size and pore ordering are the crucial parameters for kinetics of adsorption processes. Therefore, the influence of sol-gel synthesis conditions on the average size and porous structure of resulting silica particles functionalized with β-CD was analyzed. The DLS measurements were performed to evaluate the uniformity of synthesized silica particles and determine their mean hydrodynamic diameter. It was found that the behavior of CD-SiO$_2$ and CD-SiO$_2$-3 silicas at the concentration tested (0.1 mg ml$^{-1}$) is typical for uniform systems with low polydispersity indexes (Fig. 6), whereas the values of polydispersity index for CD-SiO$_2$-1 and CD-SiO$_2$-2 silicas are greater than 0.9 indicating that the samples have a very broad size distribution (Fig. 6). Obviously, introduction in template-assisted sol-gel synthesis β-CD-silane preliminarily elicited from the reaction mixture causes the formation of silica material with more uniform particles of smaller size than in the case of using the mixture obtained from β-CD-silane synthesis. As can be seen from Fig. 6, the mean diameter of silica particles calculated from the size distribution profiles increases with enhancement of β-CD:APTES molar ratio in β-CD-silane synthesis. The TEM images of β-CD-containing silicas prepared by base-catalyzed surfactant-directed sol-gel procedure are represented in Fig. 7. As can be seen, CD-SiO$_2$, CD-SiO$_2$-1, and CD-

| Silica | Polydispersity index | Diameter of particles, nm |
|---|---|---|
| CD-SiO$_2$ | 0.29 | 376 |
| CD-SiO$_2$-1 | 0.94 | 451 |
| CD-SiO$_2$-3 | 0.98 | 714 |
| CD-SiO$_2$-5 | 0.39 | 651 |

**Fig. 6** Particle size distributions for CD-SiO$_2$ (*1*), CD-SiO$_2$-1 (*2*), CD-SiO$_2$-2 (*3*), and CD-SiO$_2$-3 (*4*) determined by the DLS method

SiO$_2$-2 demonstrate particles with a highly ordered hexagonal long-range array of channels (Fig. 7a–c), whereas the quality of hexagonal arrangement of CD-SiO$_2$-3 is less defined (Fig. 7d) that may be caused by a higher content of (3-amidopropyl)triethoxysilyl groups in β-CD-silane used in organosilica synthesis. TEM images showed an average diameter of particles

up to 400 nm (Fig. 7). Relatively larger diameters calculated from DLS experiment in comparison with TEM results are due to the hydrated layer surrounding the particles with a narrow particle size distribution.

It is known that the choice of the pH values most appropriate for sorption studies is based on the stability of the silica carrier and covalent coating in aqueous solutions and is limited mainly to the pH range 2–8 (Unger 1979; Katz et al. 1998; Sagliano et al. 1988; Glajch et al. 1987; Kirkland et al. 1989). Solution acidity, in turn, affects the sorption ability of silica surface groups toward alizarin yellow because variation in pH causes changes in the protolytic state of the silica surface as well as dye molecules. However, the study of AY sorption behavior in the whole pH range suitable for silica carriers is complicated by the different solubilities of the protolytic forms of the dye. In particular, AY is very slightly soluble in water in acid medium, where carboxyl and hydroxyl groups of the dye are not ionized (Scheme 3, Fig. 8). Its aqueous solubility increases at higher pH values due to the ionization of the carboxyl group and reaches maximum in basic medium where its phenoxide form is predominant (Scheme 3, Fig. 8). Therefore, sorption studies of AY on MCM-41 and β-

**Fig. 7** TEM images of CD-SiO$_2$ (**a**), CD-SiO$_2$-1 (**b**), CD-SiO$_2$-2 (**c**), and CD-SiO$_2$-3 (**d**)



(a)

(b)

(c)

(d)
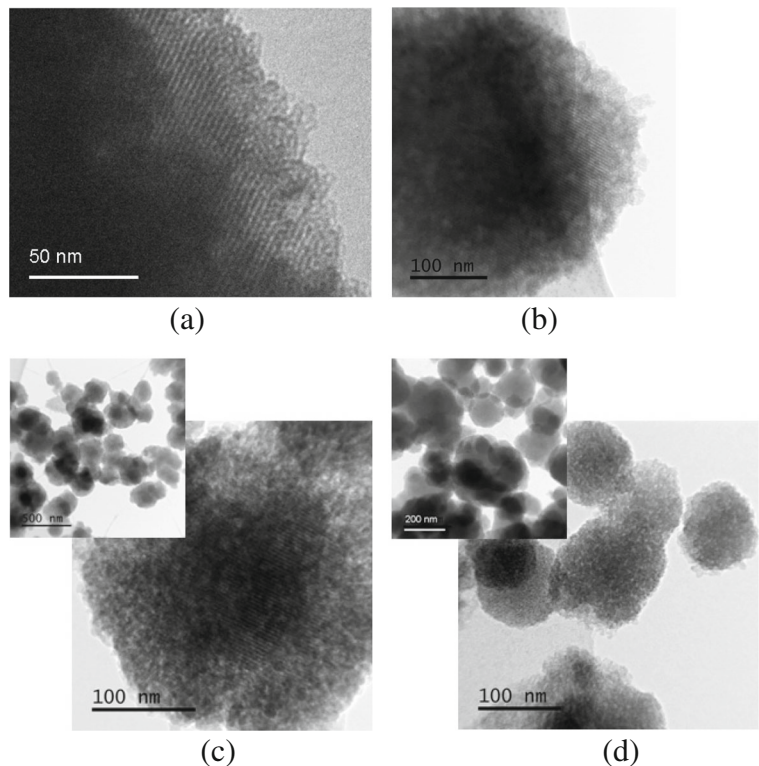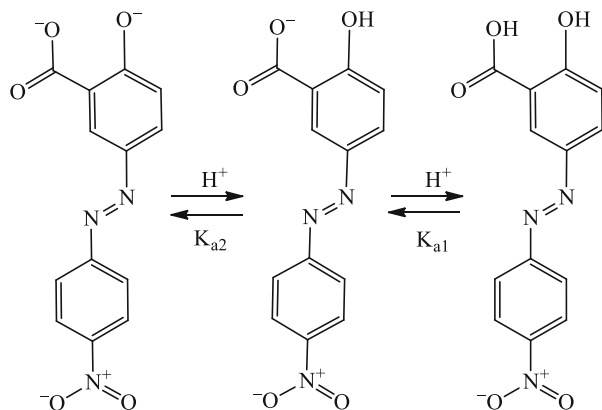
$pK_{a1}$ = 7.5 (Seleim et al. 2009)
$pK_{a2}$ = 10.5 (Seleim et al. 2009);
10.65 (Yoshida and Fujimoto 1982);
10.98 (Aoyagi et al. 1997)

**Scheme 3** Protolytic equilibria for alizarin yellow

CD-containing silica were carried out from buffer solutions with pH 7.0.

The effect of contact time on the sorption of AY on MCM-41 and CD-SiO$_2$-2 was studied at the optimum initial concentration of the dye (Fig. 9). The obtained results were analyzed using pseudo-first and pseudo-second order kinetic equations of Lagergren and Ho-McKay (Table 3), correspondingly. The agreement of experimental results and the model-predicted values is expressed by the correlation coefficient $R^2$. The low values of $R^2$ obtained for pseudo-first order kinetic model prove significant deviation of the obtained results from experimental ones (Table 3). So, the Lagergren equation is not suitable for prediction of AY sorption on synthesized silica materials. At the same time, the relatively high $R^2$ values calculated applying the pseudo-second order kinetic model indicate that the

Ho-McKay equation successfully describes the kinetics of AY sorption on MCM-41 and CD-SiO$_2$-2 (Table 3).

Sorption isotherm for AY on MCM-41 silica reaches plateau at 0.085 µmol m$^{-2}$ (Fig.10). Obviously, the key role in removing of AY by MCM-41 from neutral phosphate buffer solutions is most probably attributed to the hydrogen bonding interactions of surface silanol groups with nitrogen of azo linkage and phenolic hydroxyl groups of AY. As can be inferred from Fig. 8, close to 44% of nonionized silanol groups and 56% of ionized ones which exist at pH 7.0 are able for hydrogen bonding with nitrogen of azo linkage and hydroxyl groups of the dye, correspondingly.

Functionalization of silica surface causes a substantial rise of AY sorption in comparison with MCM-41 (Fig. 10). However, as nitrogen atom in 3-aminopropyl groups of CD-SiO$_2$-2 bears a lone electron pair, it cannot
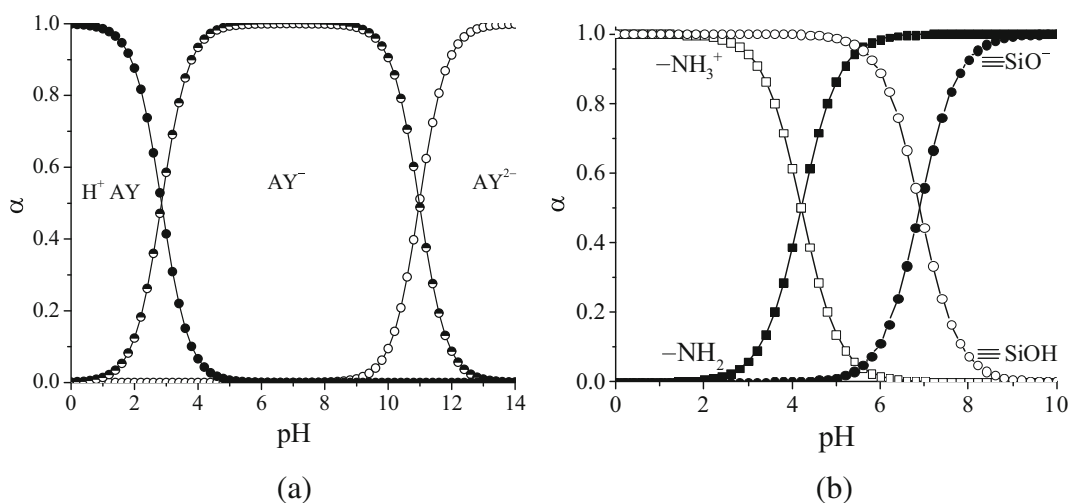


**Fig. 8** Distribution diagrams of protolytic forms of alizarin yellow (**a**) and surface silanol and aminopropyl groups of silica materials (**b**) as a function of pH
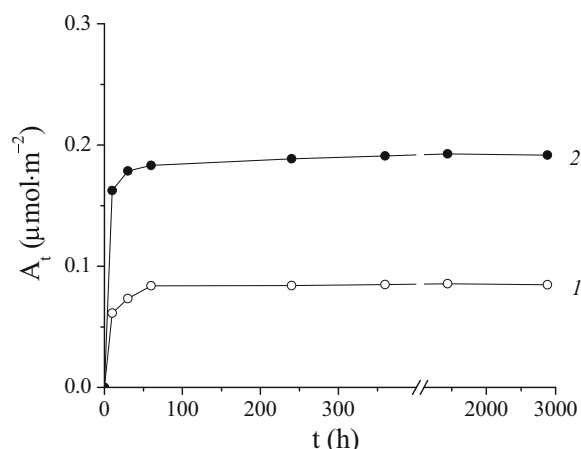
**Fig. 9** Sorption of alizarin yellow on MCM-41 (curve *1*) and CD-SiO$_2$-2 (curve *2*) at 20 °C from phosphate buffer solutions (0.323 mM) with pH 7.0 in dependence of contact time

interact with ionized carboxyl group or nitrogen of azo linkage of the dye. Moreover, its contribution to the hydrogen bonding with hydroxyl group is negligible as the value of p$K_{a2}$ for AY is too high (Pan et al. 2003). In addition, the amount by which the specific sorption increases is very close to the content of β-cyclodextrin moieties chemically immobilized on the surface of silica material. Thus, the enhancement of AY sorption uptake by CD-SiO$_2$-2 can be mainly attributed to the presence of surface cyclic oligosaccharide groups which are able to form inclusion complexes with the dye.

Equilibrium sorption data were fitted into three widely applied models, namely the Langmuir, Freundlich, and Redlich-Peterson. The Langmuir isotherm model assumes a monolayer adsorption on homogeneous sites, while the Freundlich model describes multilayer reversible adsorption on heterogeneous surface with energetically nonequivalent adsorption sites. The Redlich-

Peterson model combines the features of both the Langmuir and Freundlich equations and can predict adsorption either on homogeneous or heterogeneous sites of silica surface for which the mechanism of adsorption does not follow ideal monolayer formation. Isotherm parameters for the removal of AY from phosphate buffer solutions by silica materials are represented in Table 4. It can be seen that the values of coefficients of determination for Langmuir and Freundlich isotherm models applied for dye sorption on MCM-41 are very close and consist of 0.981 and 0.979 (Table 4), respectively. To elucidate the mechanism of AY interaction with MCM-41 silica, the nonlinear regression analysis of equilibrium adsorption by Redlich-Peterson equation was realized. It was shown that the Redlich-Peterson model is the best one for description of experimental data with coefficient of determination equal to 0.987. It can be supposed that the process of AY sorption by MCM-41 has a hybrid character due to the hydrogen bond formation between various protolytic forms of silica surface groups (nonionized and ionized silanol groups) and basic centers of AY (nitrogen of azo linkage and hydroxyl groups). Results of error analysis for AY sorption on CD-SiO$_2$-2 imply a more unambiguous description of adsorbate interaction with surface centers. The coefficients of determination estimated by the Langmuir and Freundlich models are significantly different which indicates the sorption of the dye on various surface centers of CD-SiO$_2$-2 silica. Coefficient of determination estimated using the Redlich-Peterson model has the highest value, confirming sorption of the dye on energetically nonequivalent sorption sites (silanol and β-CD-containing groups). So, comparison of the coefficients of determination and the reduced chi-squares proves that the Redlich-Peterson isotherm model is the best-fitting for equilibrium sorption of alizarin yellow on MCM-41 and CD-SiO$_2$-2 surface.

**Table 3**  Kinetic parameters for alizarin yellow sorption on MCM-41 and β-cyclodextrin-containing CD-SiO$_2$-2 silicas

| Kinetic adsorption model | Kinetic parameters | MCM-41 | CD-SiO$_2$-2 |
|---|---|---|---|
| Lagergren $\lg\left(\dfrac{A_{eq}}{A_{eq}-A_t}\right) = \dfrac{k_1}{2.303}t$   $\lg(A_{eq}-A_t) = \lg A_{eq} - \dfrac{k_1}{2.303}t$ | $k_1$ (1·min$^{-1}$) | 0.019 | 0.013 |
| | $A_{eq}$ (μmol·m$^{-2}$) | 0.025 | 0.065 |
| | $R^2$ | 0.139 | 0.555 |
| Ho-McKay $\dfrac{1}{(A_{eq}-A_t)} = \dfrac{1}{A_{eq}} + k_2 t$   $\dfrac{t}{A_t} = \dfrac{1}{k_2 A_{eq}^2} + \dfrac{1}{A_{eq}}t$ | $k_2$ (m$^2$·μmol$^{-1}$·min$^{-1}$) | 3.405 | 1.321 |
| | $A_{eq}$ (μmol·m$^{-2}$) | 0.014 | 0.044 |
| | $R^2$ | 0.829 | 0.980 |
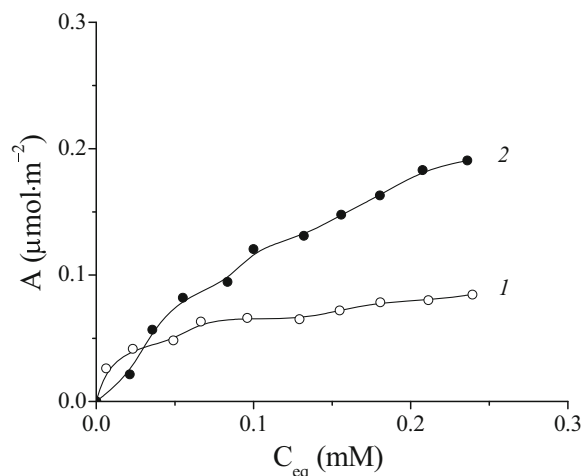
**Fig. 10** Isotherms of alizarin yellow sorption on MCM-41 (curve *1*) and CD-SiO$_2$-2 (curve *2*) at 20 °C from 0.129 to 0.323 mM phosphate buffer solutions with pH 7.0

## Conclusions

In the present work, functionalization of mesoporous silica with β-cyclodextrin groups was realized via co-condensation of tetraethyl orthosilicate with β-CD-silane prepared under mild conditions. Control under functional coverage of synthesized silica materials was achieved by using quantitative chemical,

thermogravimetric, and IR spectral analysis of their surface. Structural characteristics were estimated from the data of X-ray diffraction, low-temperature nitrogen adsorption-desorption, transmission electron microscopy, and dynamic light scattering. The obtained results verified efficient covalent attachment of β-CD moieties to the silica surface by means of amide bonds. It was found that the content of immobilized macrocyclic oligosaccharide groups depends on the structure of β-CD-silane introduced into sol-gel synthesis and increases with the number of anchoring groups. Moreover, the structure of β-CD-containing silane that takes part in co-condensation with TEOS has a substantial influence on long-range pore ordering of the resulting silica material. The formation of a highly ordered mesoporous structure was proved for organosilicas prepared by the use of β-CD-silane with equimolar quantity of anchoring (3-amidopropyl)triethoxysilyl groups. Subsequent enhancement of β-CD:APTES molar ratio in β-CD-silane synthesis leads to the lowering of pore ordering in the corresponding organosilica material.

Sorption of the dye, alizarin yellow, on MCM-41 and β-CD-containing silicas was carried out in phosphate buffer solutions with pH 7.0. Analysis of AY equilibrium sorption data was realized using Langmuir, Freundlich, and Redlich-Peterson isotherm

**Table 4** Parameters of alizarin yellow equilibrium sorption on MCM-41 and β-cyclodextrin-containing CD-SiO$_2$-2 silicas at pH 7.0

| Equilibrium adsorption model | Adsorption parameters | MCM-41 | CD-SiO$_2$-2 |
|---|---|---|---|
| Langmuir $$A_{eq} = A_m \frac{K_L C_{eq}}{1 + K_L C_{eq}}$$ $$\frac{C_{eq}}{A_{eq}} = \frac{1}{K_L A_m} + \frac{C_{eq}}{A_m}$$ | $K_L$ (1·µmol$^{-1}$) | 30.856 | 3.240 |
| | $A_m$ (µmol·m$^{-2}$) | 0.091 | 0.449 |
| | $R^2$ | 0.981 | 0.678 |
| | $\chi^2_{red}$ | 0.017 | 0.014 |
| Freundlich $$A_{eq} = K_F C_{eq}^{1/n}$$ $$\lg A_{eq} = \lg K_F + \frac{1}{n} \lg C_{eq}$$ | $K_F \cdot 10^{-3}$ (1·g$^{-1}$) | 0.132 | 0.687 |
| | $n$ | 3.178 | 1.232 |
| | $R^2$ | 0.979 | 0.938 |
| | $\chi^2_{red}$ | $5.9 \times 10^{-4}$ | $5.9 \times 10^{-3}$ |
| Redlich-Peterson $$A_{eq} = \frac{K_R C_{eq}}{1 + a_R C_{eq}^B}$$ | $K_R \cdot 10^{-3}$ (l·m$^{-2}$) | 29.396 | 1.812 |
| | $a_R$ (l·mmol$^{-1}$) | 233.822 | 4.251 |
| | $B$ | 0.721 | 0.854 |
| | $R^2$ | 0.987 | 0.991 |
| | $\chi^2_{red}$ | $1 \times 10^{-5}$ | $5 \times 10^{-5}$ |

models. Comparison of the coefficients of determination and the reduced chi-squares obtained from error analysis showed that the Redlich-Peterson isotherm model is the most appropriate for fitting the equilibrium sorption of AY on MCM-41 and β-CD-containing silicas. It was proved that oligosaccharide macromolecules localized on the surface of β-CD-containing silica contribute to the removal of AY from neutral aqueous solutions. The synthesized mesoporous silica materials with immobilized β-CD groups have promising potential in sorption, separation, and controlled delivery processes.

**Compliance with ethical standards**

**Competing interests**   The authors declare that they have no competing interests.

# References

Agrawal R, Gupta V (2012) Cyclodextrins—a review on pharmaceutical application for drug delivery. Intern J Pharm Frontier Res 2:95–112

Alahmadi SM, Mohamad S, Maan MJ (2014) Organic-inorganic hybrid materials based on mesoporous silica MCM-41 with β-cyclodextrin and its applications. Asian J Chem 26:4323–4329

Aoyagi T, Nakamura A, Ikeda H, Ikeda T, Mihara H, Ueno A (1997) Alizarin Yellow-modified β-cyclodextrin as a guest-responsive adsorption change sensor. Anal Chem 69:659–663

Bai Z-W, Lai X-H, Chen L, Ching C-B, Ng S-C (2004) Arylcarbamoylated allylcarbamido-β-cyclodextrin: synthesis and immobilization on nonfunctionalized silica gel as a chiral stationary phase. Tetrahedron Lett 45:7323–7326

Belyakov VN, Belyakova LA, Varvarin AM, Khora OV, Vasilyuk SL, Kazdobin KA, Maltseva TV, Kotvitskyy AG, Danil de Namor AF (2005) Supramolecular structures on silica surfaces and their adsorptive properties. J Coll Int Sci 285:18–26

Belyakova LA, Besarab LN, Roik NV, Lyashenko DY, Vlasova NN, Golovkova LP, Chuiko AA (2006) Designing of the centers for adsorption of bile acids on a silica surface. J Colloid Interface Sci 294:11–20

Belyakova LA, Kazdobin KA, Belyakov VN, Ryabov SV, Danil de Namor AF (2005) Synthesis and properties of supramolecular systems based on silica. J Coll Int Sci 283:488–494

Bibby A, Mercier L (2003) Adsorption and separation of water-soluble aromatic molecules by cyclodextrin-functionalized mesoporous silica. Green Chem 5:15–19

Cai K, Li J, Luo Z, Hu Y, Hou Y, Ding X (2011) β-Cyclodextrin conjugated magnetic nanoparticles for diazepam removal from blood. Chem Commun 47:7719–7721

Chen L, Zhang L-F, Ching C-B, Ng S-C (2002) Synthesis and chromatographic properties of a novel chiral stationary phase derived from heptakis(6-azido-6-deoxy-2,3-di-O-phenylcarbamoylated)-β-cyclodextrin immobilized onto aminofunctionalized silica gel via multiple urea linkages. J Chromatogr A 950:65–74

Chong ASM, Zhao XS (2003) Functionalization of SBA-15 with APTES and characterization of functionalized materials. J Phys Chem B 107:12650–12657

Concheiro A, Alvarez-Lorenzo C (2013) Chemically cross-linked and grafted cyclodextrin hydrogels: from nanostructures to drug-eluting medical devices. Adv Drug Deliv Rev 65:1188–1203

Dittert LW, Higuchi T (1963) Rates of hydrolysis of carbamate and carbonate esters in alkaline solution. J Pharm Sci 53:852–857

Dodziuk H (2006) Cyclodextrins and their complexes: chemistry, analytical methods, applications. Weinheim, Wiley-VCH

Eguchi M, Du Y-Z, Taira S, Kodaka M (2005) Functional nanoparticle based on β-cyclodextrin. NanoBiotechnology 1:165–169

Feng Y-Q, Xie M-J, Da S-L (2000) Preparation and characterization of an L-tyrosine-derivatized β-cyclodextrin-bonded silica stationary phase for liquid chromatography. Anal Chem Acta 403:187–195

Fujimura K, Ueda T, Ando T (1983) Retention behavior of some aromatic compounds on chemically bonded cyclodextrin silica stationary phase in liquid chromatography. Am Chem Soc 55:446–450

Gabbott P (2008) Princciples and applications of thermal analysis. Blackwell, Oxford

Gidwani B, Vyas A (2015) A comprehensive review on cyclodextrin-based carriers for delivery of chemotherapeutic cytotoxic anticancer drugs. Biomed Res Int 2015:1–15

Glajch JL, Kirkland JJ, Köhler J (1987) Effect of column degradation on the reversed-phase high-performance liquid chromatographic separation of peptides and proteins. J Chromatogr A 384:81–90

Gong Y, Lee HK (2003) Application of cyclam-capped β-cyclodextrin-bonded silica particles as a chiral stationary phase in capillary electrochromatography for enantiomeric separation. Anal Chem 75:1348–1354

Grun M, Unger KK, Matsumoto A, Tsutsumi K (1997) Ordered mesoporous MCM-41 adsorbents: novel routes in synthesis, product characterization and specification. In: McEnaney B, Mays JT, Rouquerol J, Rodriguez-Reynoso J, KSW S, Unger KK (eds) Characterisation of porous solids IV. The Royal Society of Chemistry, London, pp 81–89

Hegeson RC, Timko JM, Cram DJ (1973) Structural requirements for cyclic ethers to complex and lipophilize metal cations or alpha-amino acids. J Amer Chem Soc 95:3023–3025

Helfferich FG (1995) Ion exchange. Dover, New York

Hug R, Marcier L (2001) Incorporation of cyclodextrin into mesostructured silica. Chem Mater 13:4512–4519

Kaasalainen M, Aseyev V, von Haartman E, Sen Karaman D, Makila E, Tenhu H, Rosenholm J, Salonen J (2017) Size, stability, and porosity of mesoporous nanoparticles characterized with light scattering. Nanoscale Res Lett 12:74–83

Katz E, Eksteen R, Schoenmakers P, Miller N (eds) (1998) Handbook of HPLC—chromatographic science series. Marcel Dekker Inc., New York

Kawaguchi Y, Tanaka M, Nakae M, Funazo K, Shono T (1983) Chemically bonded cyclodextrin stationary phases for liquid chromatographic separation of aromatic compounds. Am Chem Soc 55:1852–1857

Kim T-W, Chung P-W, Lin VS (2010) Facile synthesis of monodisperse spherical MCM-48 mesoporous silica nanoparticles with controlled particle size. Chem Mater 22:5093–5104

Kirkland JJ, Glajch JL, Farlee RD (1989) Synthesis and characterization of highly stable bonded phases for high-performance liquid chromatography column packing. Anal Chem 61:2–11

Korenman IM (1970) Photometric analysis. Methods of determination of organic compounds. Khimia, Moscow **(in Russian)**

Kruk M, Jaroniec M (1999) Characterization of highly ordered MCM-41 silicas using x-ray diffraction and nitrogen adsorption. Langmuir 15:5279–5284

Kruk M, Sacamoto Y, Terasaki O, Ryoo R, Ko CH (2000) Determination of pore size and pore wall structure of MCM-41 by using nitrogen adsorption, transmission electron microscopy, and X-ray diffraction. J Phys Chem B 104:292–301

Lai X, Ng S-C (2003) Mono(6^A-N-allylamino-6^A-deoxy)perphenylcarbamoylated β-cyclodextrin: synthesis and application as a chiral stationary phase for HPLC. Tetrahedron Lett 44:2657–2660

Lala R, Thorat A, Cargote CS (2011) Current trends in β-cyclodextrin based drug delivery systems. IJRAP 2:1520–1526

Larkin P (2011) Infrared and Raman spectroscopy: principles and spectral interpretation. Elsevier, Oxford

Lehn JM (1978) Cryptates: inclusion complexes of macropolyciclic receptor molecules. Pure Appl Chem 50: 871–892

Lehn J-M (1995) Supramolecular chemistry: concepts and perspectives. Weinheim, VCH Verlagsgesellschaft

Li C, Song X, Hein S, Wang K (2010) The separation of GMP from milk whey using the modified chitosan beads. Adsorption 16:85–91

Li M, Tarawally M, Liu X, Liu X, Guo L, Yang L, Wang G (2013) Application of cyclodextrin-modified gold nanoparticles in enantioselective monolith capillary electrochromatography. Talanta 109:1–6

Liu C, Naismith N, Economy J (2004b) Advanced mesoporous organosilica materials containing microporous β-cyclodextrin for the removal of humic acid from water. J Chromatogr A 1036:113–118

Liu J, Alvarez J, Kaifer AE (2000) Metal nanoparticles with a Knack for molecular recognition. Adv Mater 12:1381–1383

Liu M, Da S-L, Feng Y-Q, Li L-S (2005a) Study on the preparation method and performance of a new β-cyclodextrin bonded silica stationary phase for liquid chromatography. Anal Chim Acta 533:89–95

Liu M, Li L-S, Da S-L, Feng Y-Q (2005b) High performance liquid chromatography with cyclodextrin and calixarene macrocycle bonded silica stationary phases for separation of steroids. Talanta 66:479–486

Liu Y, Han B-H, Zhang HY (2004a) Spectroscopic studies on molecular recognition of modified cyclodextrins. Curr Org Chem 8:35–46

Mondjinou YA, McCauliff LA, Kulkarni A, Paul L, Hyun S-H, Zhang Z, Wu Z, Wirth M, Storch J, Thompson DH (2013) Synthesis of 2-hydroxypropyl-β-cyclodextrin/pluronic-based polyrotaxanes via heterogeneous reaction as potential niemann-pick type C therapeutics. Biomacromolecules 14: 4189–4197

Nakanishi K (1962) Infrared adsorption spectroscopy—practical. Holden-Day, Inc., Tokyo; Nankodo Company Ltd. San Francisco

Palaniappan A, Li X, Tay FEH, Li J, Su X (2006) Cyclodextrin functionalized mesoporous silica films on quarts crystal microbalance for enhanced gas sensing. Sensors Actuators B 119:220–226

Pan BC, Xiong Y, Su Q, Li AM, Chen JL, Zhang QX (2003) Role of amination of a polymeric adsorbent on phenol adsorption from aqueous solution. Chemosphere 51:953–962

Patel P, Deshpande A (2014) Patent review on cyclodextrin based nanosponges prepared by different methods: physicochemical characterization, factors influencing formation and applications. World J Pharm Sci 2:380–385

Patil A, Chirmade UN, Trivedi V, Lamprou DA, Urquhart A, Douroumis D (2011) Encapsulation of water insoluble drugs in mesoporous silica nanoparticles using supercritical carbon dioxide. J Nanomedic Nanotechnol 2:1–8

Pedersen CJ (1967) Cyclic polyethers and their complexes with metal salts. J Amer Chem Soc 89:2495–2496

Phan TNT, Bacquet M, Laureyns J, Morcellet M (1999) New silica gels functionalized with 2-hydroxy-3-methacryloyloxypropyl-β-cyclodextrin using coating or grafting methods. Phys Chem Chem Phys 1:5189–5195

Phan TNT, Bacquet M, Morcellet M (2000) Synthesis and characterization of silica gels functionalized with monochlorotriazinyl β-cyclodextrin and their sorption capacities towards organic compounds. J Incl Phenom Macrocycl Chem 38:345–359

Roik NV, Belyakova LA (2013) Sol-gel synthesis of MCM-41 silicas and selective vapor-phase modification of their surface. J Solid State Chem 207:194–202

Roik NV, Belyakova LA (2011) Interaction of supramolecular centers of silica surface with aromatic amino acids. J. Colloid Interface Sci 362: 172–179

Sagliano N Jr, Hartwick RA, Patterson RE, Woods BA, Bass JL, Miller NT (1988) Stabilization of reversed phases for liquid chromatography: application of infrared spectroscopy for the study of bonded-phase stability. J Chromatogr A 458:225–240

Salis A, Casula MR, Bhattacharyya MS, Pinna M, Solinas V, Monduzzi M (2010) Physical and chemical lipase adsorption on SBA-15: effect of different interactions on enzyme loading and catalytic performance. Chem Cat Chem 2:322–329

Schneiderman E, Stalcup AM (2000) Cyclodextrins: a versatile tool in separation science. J Chromatogr B 745:83–102

Seleim MM, Abu-Bakr MS, Hashem EY, El-Zohry AM (2009) Simultaneous determination of aluminum (III) and iron (III) by first-derivative spectrophotometry in alloys. J Appl Spectrosc 76:554–563

Shpigun OA, Ananieva IA, Budanova NY, Shapovalova EN (2003) Use of cyclodextrins for separation of enantiomers. Russ Chem Rev 72:1035–1054

Shvets O, Belyakova L (2015) Synthesis, characterization and sorption properties of silica modified with some derivatives of β-cyclodextrin. J Hazard Mat 283: 643−656.

Staab HA (1962) Syntheses using heterocyclic amides (azolides). Angew Chem Int Ed Engl 1:351–367

Steed JW, Atwood JL (2009) Supramolecular chemistry. Wiley, New York

Stuart BH (2004) Infrared spectroscopy: fundamentals and applications. Wiley, Chichester

Szejtli J (1998) Introduction and general overview of cyclodextrin chemistry. Chem Rev 98:1743–1753

Tiwari G, Tiwari R, Rai AK (2010) Cyclodextrins in delivery systems: applications. J Pharm Bioallied Sci 2:72–79

Unger KK (1979) Porous silica—its properties and use as support in column liquid chromatography. Elsevier, Amsterdam

Xu X, Liu Z, Zhang X, Duan S, Xu S, Zhou C (2011) β-Cyclodextrin functionalized mesoporous silica for electrochemical selective sensor: simultaneous determination of nitrophenol isomers. Electrochim Acta 58:142–149

Yano H, Hirayama F, Arima H, Uekama K (2001) Preparation of prednisolone-appended α-, β- and γ-cyclodextrins: substitution at secondary hydroxyl groups and in vitro hydrolysis behaviour. J Pharm Sci 90:493–503

Yoshida N, Fujimoto M (1982) Proton-transfer reactions of 5-(m- and p-nitrophenylazo)salicylic acids coupled with inclusion reactions with α- and β-cyclodextrins. Bull Chem Soc Jpn 55:1039–1045

Zhang L-F, Wong Y-C, Chen L, Ching CB, Ng S-C (1999) A facile immobilization approach for perfunctionalised cyclodextrin onto silica via the Staudinger reaction. Tetrahedron Lett 40:1815–1818